

# Internal modified-layer formation mechanism into silicon with nanosecond laser

E. Ohmura <sup>a,\*</sup>, F. Fukuyo <sup>b</sup>, K. Fukumitsu <sup>b</sup>, H. Morita <sup>b</sup>

<sup>a</sup> Division Materials and Manufacturing Science, Osaka University,  
2-1, Yamada-Oka, Sita, Osaka, Japan

<sup>b</sup> Hamamatsu Photonics K. K., 314-5, Shimo-Kanzo, Iwata, Shizuoka, Japan

\* Corresponding author: E-mail address: ohmura@mape.eng.osaka-u.ac.jp

Received 15.03.2006; accepted in revised form 30.04.2006

## Manufacturing and processing

### ABSTRACT

**Purpose:** When a permeable nanosecond pulse laser which is condensed into the inside of a silicon wafer is scanned in the horizontal direction, a belt-shaped polycrystal layer is formed at an arbitrary depth in the wafer. Applying tensile stress perpendicularly to this belt-shaped modified-layer, silicon wafer can be separated easily into individual chip without creating any damage to the wafer surface comparing with the conventional blade dicing method, because the cracks that spread from the modified layer up and down progress to the surface. This technology is called “stealth dicing” (SD), and attracts attentions as a novel dicing technology in semiconductor industries. The purpose of this study is to clarify the formation mechanism of modified layer.

**Design/methodology/approach:** We paid attention to an experimental result that the absorption coefficient varies with temperature. We analyzed a coupling problem composed of condensed laser propagation in a silicon single crystal, laser absorption, temperature rise, and heat conduction. Simple thermal stress analysis was also conducted based on those results.

**Findings:** As a result, formation mechanism of the modified layer could be explained clearly. Temperature dependence of absorption coefficient is the most important factor of the modified layer formation.

**Research limitations/implications:** The present analysis can be applied to find the optimum laser irradiation condition for SD method, and it is a future subject to confirm it experimentally.

**Practical implications:** It was supported by the present analysis that the problem of thermal effect on the active region can be solved by the SD method.

**Originality/value:** SD method for wafer dicing is original firstly and it is valuable that formation mechanism of the modified layer in SD method was clarified theoretically.

**Keywords:** Machining; Laser dicing; Silicon; Internal modification

## 1. Introduction

When a permeable nanosecond laser which is condensed into the inside of a silicon (Si) wafer is scanned in the horizontal direction as shown in Fig. 1 schematically, a belt-shaped polycrystal layer is formed in the wafer and cracks progress from polycrystal region to monocrystal area. When tensile stress is applied perpendicularly to this belt-shaped modified-layer, Si wafer can be divided easily, because the cracks that

spread from the modified layer up and down progress to the surface. This technology is called “stealth dicing” (SD), and attracts attentions as a novel dicing technology in semiconductor industries [1].

Mechanical cutting with a dicing saw has been mainly used conventionally for dicing of Si wafer [2-5]. This is wet process, and pollution of devices is fatal [6]. In addition, chipping and microcracks which occur in cut end-faces become problems from the standpoint of transverse intensity [7]. It is also unfavorable from the point of view of yield rate that its kerf is relatively large.

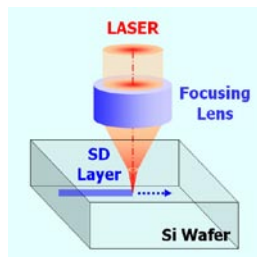


Fig. 1. Schematic of stealth dicing

On the other hand, laser dicing using laser ablation [8, 9] or laser thermal breaking have been used, too [10-14]. Influence of heat and debris pollution generated in laser processing on device property and reliability cannot be ignored, as a laser of the wavelength that Si is easy to absorb is adopted in such laser dicing. In addition, end face accuracy in the laser thermal breaking method and microcracks generated in the laser ablation method are also problems, respectively.

As for the SD method, a laser beam propagates to the neighborhood of the focal point in the wafer, because a wavelength permeable for Si is used. On this account there is no damage at the surface layer of a wafer where actual devices are formed. Moreover the debris pollution and thermal effect at the active domain, which are the problems in the conventional laser dicing technologies, can be solved by the SD method, therefore, it can be considered that the SD method has much larger advantage. Therefore the SD method can be regarded as a superior processing method, but it is necessary to clarify the formation mechanism of the internal modified-layer in order to establish it as a dicing technology with higher reliability and investigate the optimum processing conditions. It is the purpose of this study to clarify the internal modified-layer formation mechanism by a heat conduction analysis in which the temperature dependence of absorption coefficient is considered and an easy thermal stress analysis.

## 2. Absorption model of condensed gaussian beam

1,064 nm laser is supposed here, and an internal temperature rise of Si by single pulse irradiation is analyzed. Considering that a laser beam is axisymmetric, we introduce the cylindrical coordinate system  $O-rz$  whose  $z$ -axis corresponds to the optical axis of laser beam and  $r$ -axis is taken on the surface of Si. Absorption coefficient  $\mu(T_{i,j})$  in a lattice  $(i, j)$  whose temperature is  $T_{i,j}$  is expressed by  $\mu_{i,j}$ . When Lambert law is applied between a small depth  $\Delta z$  from depth  $z = z_{j-1}$  to  $z = z_j$ , laser intensity  $I'_{i,j}$  at the depth  $z = z_j$  is expressed by

$$I'_{i,j} = I_{i,j} e^{-\mu_{i,j} \Delta z}, \quad (1)$$

where  $I_{i,j}$  is laser intensity at the depth  $z = z_{j-1}$ .

The  $1/e^2$  radius at the depth  $z$  of a laser beam which is condensed with a lens is expressed by  $r_e(z)$ . In propagation of light waves from the depth  $z = z_{j-1}$  to  $z = z_j$ , condensing or divergence of a beam can be evaluated by a parameter

$$\gamma_j = r_e(z_j) / r_e(z_{j-1}). \quad (2)$$

A beam is condensed when  $\gamma_j$  is less than 1, and is diverged when  $\gamma_j$  is larger than 1. Now, laser intensity  $I_{i,j}$  at the depth  $z = z_{j-1}$  of a finite difference grid  $(i, j)$  can be expressed by the energy conservation as follows:

(1) For  $\gamma_{j-1} < 1$

$$I_{i,j} = \frac{(\gamma_{j-1}^2 r_i^2 - r_{i-1}^2) I'_{i,j-1} + (1 - \gamma_{j-1}^2) r_i^2 I'_{i+1,j-1}}{\gamma_{j-1}^2 (r_i^2 - r_{i-1}^2)}. \quad (3)$$

(2) For  $\gamma_{j-1} > 1$

$$I_{i,j} = \frac{(\gamma_{j-1}^2 - 1) r_{i-1}^2 I'_{i-1,j-1} + (r_i^2 - \gamma_{j-1}^2 r_{i-1}^2) I'_{i,j-1}}{\gamma_{j-1}^2 (r_i^2 - r_{i-1}^2)}. \quad (4)$$

Considering Eq. (1), internal heat generation per unit time and unit volume in the grid  $(i, j)$  is given by

$$w_{i,j} = (1 - e^{-\mu_{i,j} \Delta z}) I_{i,j} / \Delta z. \quad (5)$$

## 3. Analysis results and discussion

Concrete analysis was conducted under the irradiation condition shown in Table 1. Pulse energy  $E_p$  is effective value to penetrate Si. Pulse width  $\tau_p$  is defined with FWHM. Time of pulse center is assumed  $t = 0$ . The intensity distribution of a beam was assumed to be Gaussian. It was supposed that the thickness of single crystal Si is 100  $\mu\text{m}$  and the depth of focal plane  $z_0$  is 60  $\mu\text{m}$ . The initial temperature is 293 K.

The analysis region of Si was a disk such that the radius is 100  $\mu\text{m}$  and the thickness is 100  $\mu\text{m}$ . In the numerical calculation, an inside of the radius of 20  $\mu\text{m}$  was divided into 400 at 50 nm evenly, and its outside region was divided into 342 by logarithmic grid. The thickness was divided into 10,000 at 10 nm evenly in the depth direction. The time step was 20 ps. The boundary condition was assumed insulation.

When the temperature dependence of absorption coefficient was taken into account, time variation of temperature distribution along the central axis is shown in Fig. 2. It can be understood from these figures that laser absorption begins suddenly in the neighborhood of the depth  $z = 59 \mu\text{m}$  at about  $t = -45 \text{ ns}$  and the temperature rises to about 20,000 K instantaneously.

Table 1  
Irradiating condition

Pulse energy $E_p$	4.45 $\mu\text{J}$
Pulse width $\tau_p$	150 ns
Depth of focal plane $z_0$	60 $\mu\text{m}$
Spot radius $r_0$	485 nm

The region where the temperature rises beyond 10,000 K will be instantaneously vaporized and a void is formed. After that high temperature area expands rapidly in the surface direction as shown in Fig. 3. Time variation of heating rate at various depths along the central axis is shown in Fig. 4. Heating or cooling rate was calculated by

$$\dot{T}_{i,j}(t) = [T_{i,j}(t) - T_{i,j}(t - \Delta t)] / \Delta t \quad (6)$$

with  $\Delta t = 5 \text{ ns}$ .

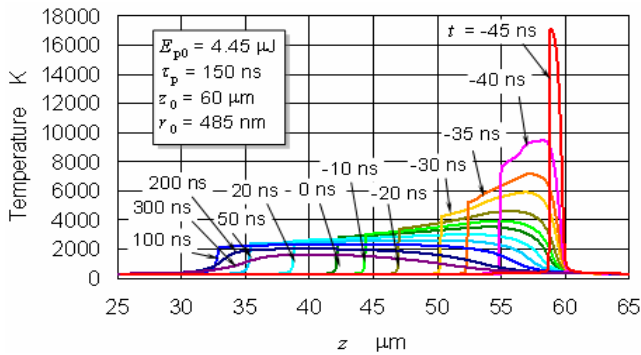


Fig. 2. Time variation of temperature distribution along the central axis

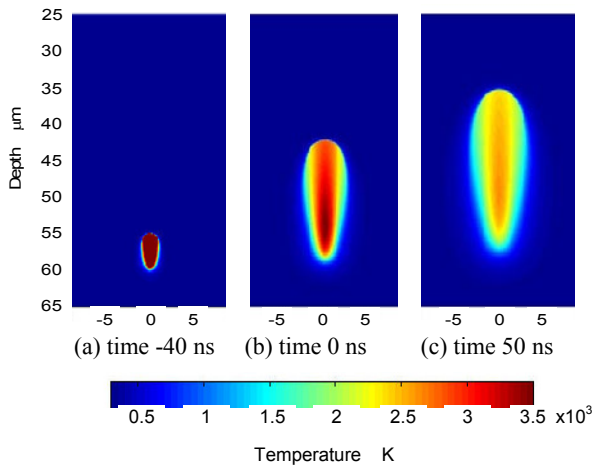


Fig. 3. Time variation of temperature distribution

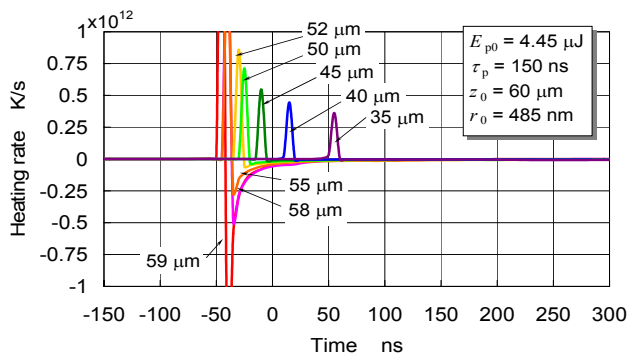


Fig. 4. Time variation of heating rate at various depths along the central axis

Momentary maximum temperature gradually falls. Temperature decline at the depth of 55 μm to 60mm is particularly notable. The maximum cooling rate at this neighborhood is about 10<sup>12</sup> K/s (see Fig. 4). Laser is always absorbed at the vicinity of leading edge of the high temperature region, yielding a thermal shock wave. Time variation of the position where temperature rises to 1,000K is shown in Fig. 5. This expresses time variation of a leading edge of thermal shock

wave during heating. It is understood that the thermal shock wave travels at mean speed of about 250 m/s. Cooling rate at the area of 53 μm to 33 μm in depth gradually decreases from 10<sup>11</sup> K/s to 10<sup>8</sup> K/s, but it is still rapid cooling.

Very large temperature difference occurs between the high-temperature region by laser absorption and its circumference as understood from Fig. 3. Because thermal expansion of the high-temperature region is immobilized by the neighboring low-temperature region, the high temperature region must receive very strong compression. Therefore this compressive stress was estimated simply by

$$\sigma = E\alpha\Delta T / (1 - \nu), \quad (7)$$

where  $E$  is Young's modulus,  $\alpha$  is linear expansion coefficient,  $\Delta T$  is temperature difference between the maximum temperature and the initial temperature and  $\nu$  is Poisson's ratio. It is understood that a super high pressure state of about 12 GPa is generated at the early stage when laser absorption becomes notable.

In Fig. 5, compressive stress already decreases below 5 GPa at time -35 ns, and after that falls rapidly with decrease of the maximum temperature. At the same time, the position of the maximum compressive stress gradually moves to the surface side with progress of thermal shock wave.

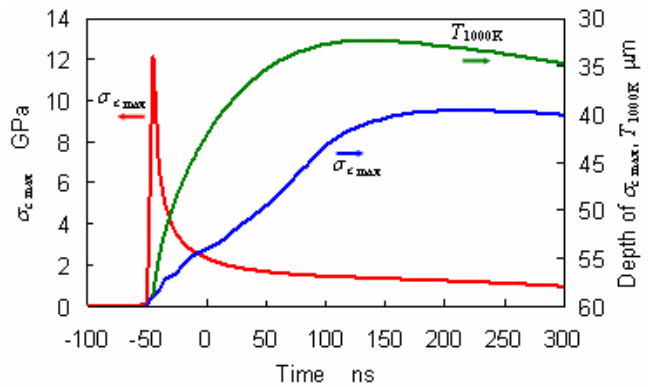


Fig. 5. Time variations of the maximum compressive stress along the central axis, its depth and the position where temperature rises to 1000 K

Thus far compressive stress was estimated by Eq. (7). Actually heating rate is large in the vicinity of the leading edge of thermal shock wave as had shown by Fig. 4, and compressive stress acts strongly on this domain. The area that the leading edge of thermal shock wave passed will turn into a tensile stress state from a compressive stress state quickly, because cooling rate at that area is relatively large as have been seen in Fig. 4. As a result, melting can progress in cooling process although it was restrained for strong compressive stress during heating, then solidification and polycrystallization will occur with further temperature fall.

Maximum temperature distribution is shown in Fig. 6 (a). The area where temperature reaches over 1,690 K which is the melting point under atmospheric pressure [15] is shown by binarization in Fig. 6 (b). Figure 7 (a) shows a schematic of a modified layer based on its formation mechanism estimated as a result of this study. Figure 7 (b) is a photograph of the cross section of SD processed Si wafer. A pulse laser was irradiated from the upper direction of the photograph, and scanned in the

transverse direction. The central band-shaped region is the modified layer. The experimental result can be explained well by thinking that the modified layer shown by the schematic of Fig. 8 (a) was generated by every pulse irradiation.

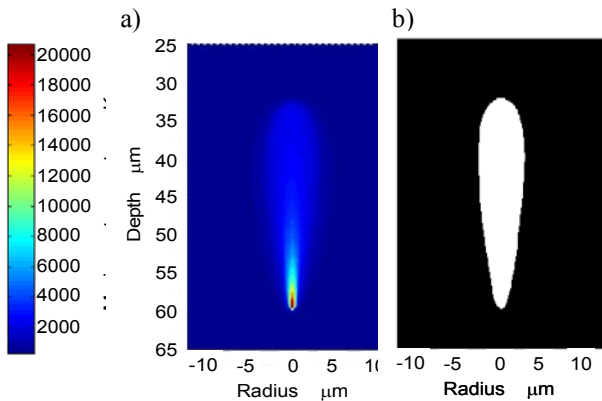


Fig. 6. Maximum temperature distribution (a) and area reached above usual melting point (b)

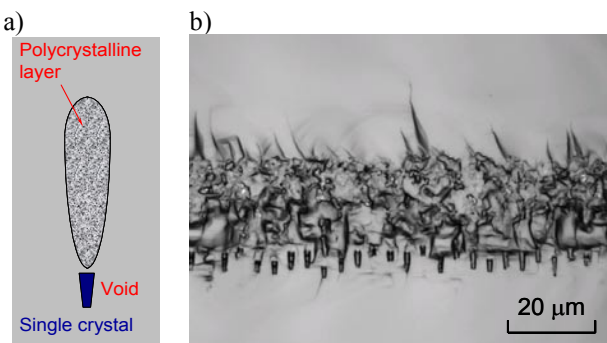


Fig. 7 Schematic of modified layer (a) and example of experimental result (b)

## 4. Conclusions

In the stealth dicing (SD) method, a laser beam which usually penetrates is absorbed locally at the vicinity of a focal point inside of a Si wafer, and the modified layer composed of void and polycrystal layer (SD layer) is generated. In this paper, formation mechanism of the modified layer was explained by the heat transfer analysis in which the temperature dependence of absorption coefficient is considered and simple thermal stress analysis based on those results. The main conclusions can be summarized as follows: For temperature dependence of absorption coefficient, laser absorption occurs suddenly at the vicinity of the focal point inside of Si single crystal. Void is generated suddenly at the early stage of laser absorption, and a thermal shock wave propagates afterwards to the surface direction. The vicinity of the leading edge of thermal shock wave is very strongly compressed. Melting and evaporation are

restrained under super high compression at the heating stage, and melting and polycrystallization by solidification occur during cooling period after the leading edge of thermal shock wave passed.

## References

- [1] F. Fukuyo, K. Fukumitsu and N. Uchiyama: The Stealth Dicing Technologies and Their Application, Proceedings of 6th Laser Precision Microfabrication, (2005).
- [2] J. Ikeno, Y. Tani and A. Fukutani: Development of Chipping-Free Dicing Technology Applying Electrophoretic Deposition of Ultrafine Abrasives, Annals of CIRP 41/1 (1992) 351-354.
- [3] W. Peng, X.F. Xu and L.F. Zhang: Improvement of a Dicing Blade Using a Whisker Direction-Controlled by an Electric field, Journal of Materials Processing Technology 129 (2002) 377-379.
- [4] I.-H. Cho, S.-C. Jeong, J.-M. Park and H.-D. Jeong: The Application of Micro-Groove Machining for the Model of PDP Barrier Ribs, Journal of Materials Processing Technology 113 (2001) 355-359
- [5] S.B. Lee, Y. Tani, H. Ssato and T. Enomoto: Development of a Dicing Blade with Photopolymerizable Resins for Improving Machinability, Annals of CIRP 54/1 (2005) 293-296.
- [6] G.C. Lim, A.T. Mai, D. Low and Q. Chen: High Quality Laser Microcutting of Difficult-to-Cut Materials - Copper and Si Wafer, Proceedings of 21st International Congress on Applications of Lasers and Electro-Optics, (2002).
- [7] R. Ebutt, S. Danyluk and I. Weisshaus: Method to Evaluate Damage Induced by Dicing and Laser Cutting of Si Wafers, Microstructural Science 23 (1996) 89-94.
- [8] Y. Ishizaka, I. Fukumoto, E. Ohmura and I. Miyamoto: Three-Dimensional Molecular Dynamics Simulation on Laser Materials Processing of Silicon, Proceedings of 17th International Conference on Applications of Lasers and Electro Optics 85, Sec. A (1998) 55-63.
- [9] K. Watanabe, Y. Ishizaka, E. Ohmura and I. Miyamoto: Analysis of Laser Ablation Process in Semiconductor Due to Ultrashort Pulsed Laser with Molecular Dynamics Simulation, Proceedings of SPIE 3933 (2000) 46-55.
- [10] T. Corboline, C.E. Rea and C. Dunskey: High Power UV Laser Machining of Si Wafers, Proceedings of SPIE 5063, Fourth International Symposium on Laser Precision Microfabrication, (2003), 495-500.
- [11] T. Lizotte: Laser Dicing of Chip Scale and Silicon Wafer Scale Packages, Proceedings of IEEE/CMPT/SEMI Int'l Electronics Manufacturing Technology Symposium (2003) 1-5.
- [12] M. Li: Effect of Laser Parameters on Semiconductor Micromachining Using Diode-Pumped Solid-State Lasers, Proceedings of 21st International Congress on Applications of Lasers and Electro-Optics, LMF Sec. B (2003) 7-15.
- [13] D. Perrottet, A. Spiegel, F. Wagner, R. Housh, B. Richerzhagen and J. Manley: Particle-free Semiconductor Dicing Using the Water Jet Guided Laser Technology, Proceedings of 21st International Congress on Applications of Lasers and Electro-Optics (2004).
- [14] P. Chall: ALSI's Low Power Multiple Beam Technology for High Throughput and Low Damage Wafer Dicing, Proceedings of 65th Laser Materials Processing Conference, (2005), 211-215.
- [15] S.P. Parker, et al. ed.: Dictionary of Physics, 2nd ed. (1997) McGraw-Hill.